A Novel Technique for the Approximation of 3-D Antenna Radiation Patterns

Theodore G. Vasiliadis, *Student Member, IEEE*, Antonis G. Dimitriou, *Student Member, IEEE*, and George D. Sergiadis, *Member, IEEE*

***Abstract*—In this paper, a novel technique for the approximation of three-dimensional (3-D) antenna radiation patterns is presented. The proposed method combines the two principal cuts in order to acquire an adequate estimate of the 3-D antenna radiation solid. The absolute error from the theoretical solution is analyzed along with other statistical measures for various types of antenna structures, namely omni-directional and directive arrays. The performance of the method is compared against other existing extrapolation algorithms. The proposed technique exhibits low approximation errors and is easily integrated into 3-D radio propagation planning tools (such as ray-tracing algorithms).**

***Index Terms*—Antenna radiation patterns, approximation methods, prediction methods, radio propagation.**

I. Introduction

THE complexity of modern wireless network design has led operators to focus on new ways and means by which wireless services will evolve and overcome difficulties related to signal propagation inside buildings and dense urban environments. Accurate propagation prediction is needed in such cases, in order to provide high-quality services with maximum availability. High-resolution prediction techniques [full three-dimensional (3-D)] are generally preferred, implementing deterministic models for signal propagation, since classical empirical models have been proved deficient in accuracy, when used in dense environments where most of the traffic is situated.

Prediction accuracy in deterministic planning tools depends mainly on building/terrain modeling and on the constitutive parameters of building-materials. Moreover, most antenna manufacturers provide information only about the two principal radiation cuts (azimuth/elevation) of the antenna used in the simulation. Since the 3-D pattern is apparently needed, an estimate of the radiation solid is extrapolated from the horizontal and vertical patterns. The overall degradation in accuracy of the predicted signal strength depends on the reconstruction algorithm being employed.

The most evident way of approximating the 3-D radiation pattern from its two principal cuts, is probably by summing the available samples for each azimuth and elevation angle (assuming decibel values). This classic method is still used in many planning tools, when 3-D capabilities are required, and will be thoroughly examined in Sections II–VII for the purpose of comparison. The main advantage besides the simplicity of the method is the fact that normalized omni-directional patterns (as defined in IEEE Std.145-1993) are perfectly reconstructed, because of their inherent axial symmetry. In that case, the radiation solid is given simply by rotating the elevation pattern for all azimuth angles.

Early work on the subject has been also reported in [1], where a variation of the traditional elliptical-fit algorithm has been used for reconstruction from two planar patterns. In the case of omni antennas, predefined textbook equations are used to model the elevation pattern, since the elliptical-fit algorithm cannot adequately reconstruct this type of patterns. The application of the method is therefore limited to directive antennas only, where the boresight shall be aligned to one of the planar samples. The accuracy is constrained due to the inability of the designed algorithm to distinguish any sidelobes (that fall in either the azimuth or elevation pattern) from the mainlobe [1].

Other work is reported in [2], [3] where the interpolated gain is calculated by weighting four known sample points (belonging to horizontal or vertical cut) closest to the point of interest, depending on the angular distance from each sample. The algorithm takes into account both sides of the vertical cut (front and back—360 values), information that is not always available by antenna manufacturers. The technique exhibits moderate accuracy for a fairly directive two-element dipole array, but does not examine the case of highly directive base-station antennas. Furthermore, the main disadvantage of this interpolation method is the inability to precisely reconstruct omni-directional patterns, compared to the aforementioned summing algorithm (SA). In the case of a half-wavelength dipole, a maximum deviation of 12 dB between interpolated and theoretical patterns is reported.

The use of model-based parameter estimation (MBPE) algorithms is proposed in [4] and further extended in [5], for interpolating radiation patterns both in spatial and spectral domain. The goal of this method though, is to minimize the number of samples required to accurately reproduce planar patterns (at any desired frequency), rather than reconstructing the radiation solid in its whole.

An empirical formula for the generation of 3-D antenna patterns was presented in [6], but no statistical measures have been reported to evaluate its performance. Finally, typical mathematical interpolation methods (like cubic splines or rational functions) have been used in [7] to approximate the 3-D pattern by a limited set of measured planar sample-cuts. The performance of the developed algorithm was evaluated by simply comparing patterns approximated by a different number of interpolated samples, instead of directly comparing with the theoretical antenna pattern.

In this paper, a novel technique for the 3-D pattern reconstruction from only the azimuth and elevation cuts will be presented

Manuscript received November 10, 2004; revised January 13, 2005.

The authors are with the Aristotle University of Thessaloniki, Faculty of Engineering, Department of Electrical and Computer Engineering, Telecommunications Laboratory, Thessaloniki GR54124, Greece (e-mail: sergiadi@auth.gr).

Digital Object Identifier 10.1109/TAP.2005.850752

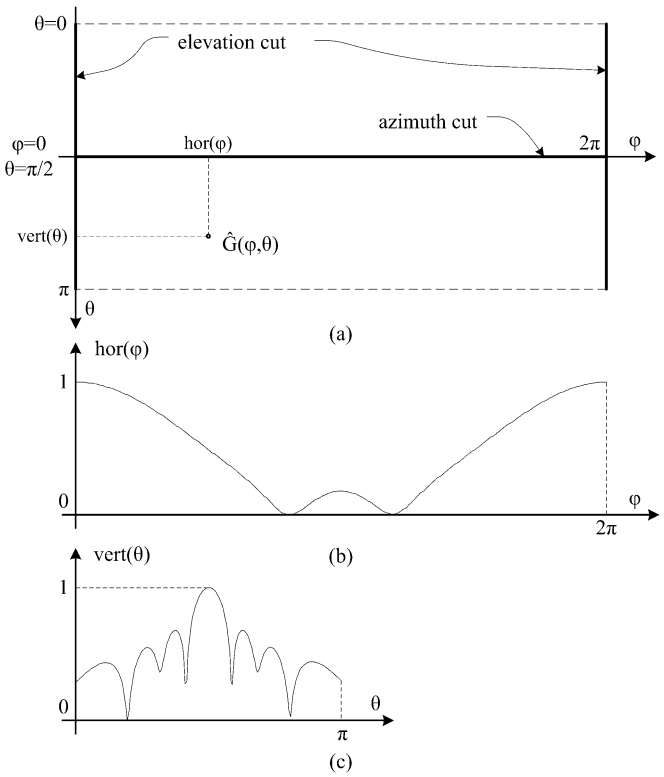

Fig. 1. (a) Planar projection of the antenna's surrounding sphere, with associated radiation cuts. (b) Examples of horizontal and (c) vertical radiation pattern for Kathrein 739 490 base-station flat-panel antenna.

in detail. The main concept behind the proposed method will be discussed at first, and several case studies will be investigated in order to assess its overall performance. The versatility of the developed algorithm enables its use in cases of both omni and directive antennas with increased accuracy. In fact, when axially symmetric (omni) patterns are used, the approximation error is zero, as in the classic summing algorithm. A statistical evaluation of the accuracy for both cases will be also presented. Finally, a generalized, hybrid method will be introduced and discussed, that minimizes the achieved approximation error.

II. Proposed Approximation Algorithm

The proposed reconstruction technique combines the two principal normalized patterns, namely the azimuth (horizontal) and elevation (vertical) cut, using 360 horizontal and 180 vertical gain samples. As illustrated in Fig. 1, the azimuth pattern is actually the planar cut at $\vartheta = \pi/2$ while the vertical pattern is the cut at $\varphi = 0$ (which is identical to $[\varphi = 2\pi]$). Example decimal gain patterns are depicted in Fig. 1(b) and (c) abbreviated as $\mathrm{hor}(\varphi)$ and $\mathrm{vert}(\vartheta)$ respectively. We define as G_H and G_V their corresponding logarithmic counterparts (in decibels), i.e., $G_H(\varphi) = 10 \cdot \log[\mathrm{hor}(\varphi)]$ and $G_V(\vartheta) = 10 \cdot \log[\mathrm{vert}(\vartheta)]$.

At an arbitrary point (φ, ϑ), the approximated antenna gain $\widehat{G}$ is calculated by weighting the horizontal/vertical samples (at the point of interest), according to the following formula:

$$\widehat{G}(\varphi,\vartheta) = \frac{G_H(\varphi)\cdot w_1 + G_V(\vartheta)\cdot w_2}{\sqrt[k]{w_1^k + w_2^k}} \tag{1}$$

where k is a normalization-related parameter (discussed later), while the weight functions w_1 and w_2 are given by

$$\begin{aligned} w_1(\varphi,\vartheta) &= \mathrm{vert}(\vartheta)\cdot[1-\mathrm{hor}(\phi)] \\ w_2(\varphi,\vartheta) &= \mathrm{hor}(\phi)\cdot[1-\mathrm{vert}(\vartheta)]. \end{aligned} \tag{2}$$

The main concept behind this technique is that the estimation process of a radiation sample involves the actual data of the other principal pattern, as a function of angular distance between the point of interest and the sample, in a cross-weighting manner between the two principal cuts. This is proved to be more efficient than other interpolation schemes with linear or exponential angular distance dependency.

In the proposed approach, the weighting function has a two-fold character: It provides with the means for appropriate angular distance weighting, and also takes into account the physics of propagation. In the proposed concept, the reconstruction problem is not treated as a purely mathematical extrapolation problem, but instead the physical properties of the radiation pattern are used to improve accuracy and minimize the uncertainty of the interpolated gain. As a characteristic example, in the proposed technique the radiation nulls contribute differently in the gain estimation. In directions of lower radiated energy (nulls) on both principal patterns, where maximum estimation uncertainty is expected, the proposed approximation method assigns different significance to each null, rather than cumulating their effect.

Moreover, the initial weights being employed in this process, are subjected to further shaping in (2), by the terms in brackets. These terms define, in some extent, the significance of the initial weights related to the angular distance between the point of interest and the sample. This is done again by cross-shaping between the two principal cuts, but in an inverse manner (unitary complements). For example, at a point $P(\varphi_1, \vartheta_1)$ the sample $G_H(\varphi_1)$ is weighted by $\mathrm{vert}(\vartheta_1)$ (due to P's angular distance ϑ_1 from the $\vartheta = \pi/2$ sample-cut), which in turn is shaped by $[1 - \mathrm{hor}(\varphi_1)]$ (due to P's distance φ_1 from the $\varphi = 0$ weight sample-cut).

We define as A_1 and A_2 the overall normalized weights of the two sample radiation cuts according to

$$\begin{aligned} \widehat{G}(\varphi,\vartheta) &= G_H(\varphi)\cdot\frac{w_1}{\sqrt[k]{w_1^k + w_2^k}} + G_V(\vartheta)\cdot\frac{w_2}{\sqrt[k]{w_1^k + w_2^k}} \\ &= G_H(\varphi)\cdot A_1 + G_V(\vartheta)\cdot A_2. \end{aligned} \tag{3}$$

Since $A_1,\ A_2 \in [0,1]$ and $G_H,\ G_V \leq 0\ \forall\ (\varphi,\vartheta)$, it is apparent that $G_{\mathrm{SA}}(\varphi,\vartheta) = G_H(\varphi) + G_V(\vartheta) \leq \widehat{G}(\varphi,\vartheta) \leq 0$ for all azimuth and elevation angles, where the classic summing algorithm is denoted by G_{SA}. That is, the proposed approximation method is generally a more "optimistic" (= offering higher estimation values) approach compared to the summing algorithm.

The initial weights stated in (2) are normalized in the approximation formula by the denominator of (1), so that the following relationship between A_1 and A_2 is met:

$$A_1^k + A_2^k = 1. \tag{4}$$

The weights A_1, A_2 define mathematically the degree of participation of each sample-cut into the overall approximation, as shown in (3). In a way, they also define the divergence of the proposed method from the summing algorithm, which in fact can

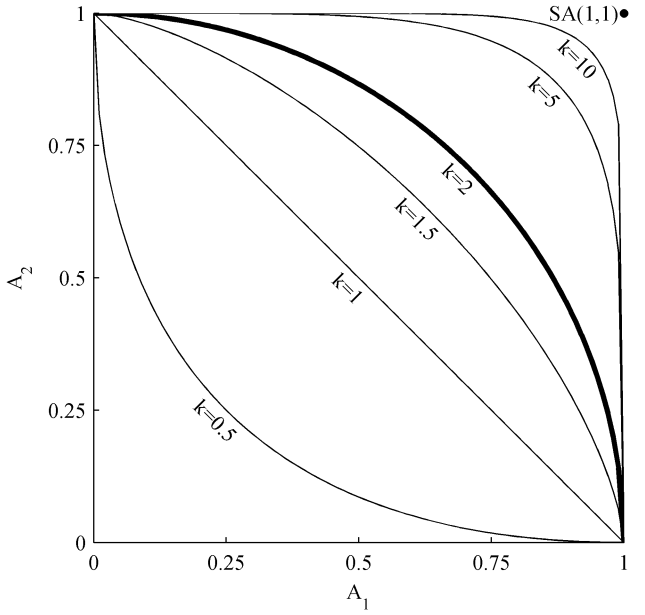

Fig. 2. Geometrical locus of normalized weights A_1 and A_2 for different parameters k. Point (1,1) represents the special case of the summing algorithm (SA). Bold line corresponds to the optimum parameter $(k = 2)$ used in the proposed method.

be considered a special case of this formulation if $A_1 = A_2 = 1$ is applied to (3). In the proposed approach, the relationship between the normalized weights can be selected from the family of curves defined in (4). The geometrical locus of these weights for various parameters k is depicted in Fig. 2. Note that the point (1,1) is actually the case of the summing algorithm. By increasing the normalization parameter k, the proposed method tends to an increasingly "pessimistic" solution.

In a typical normalization procedure, the sum of weights A_1 and A_2 is equal to $1(k = 1)$, hence the locus is a linear segment. However, a parametric study for k has proved that an optimum value of $k = 2$ yields a minimum approximation error, for all antennas considered herein. Therefore, the geometrical locus of the normalized weights is a sector of a unit-circle. This condition $(k = 2)$ will be considered during all simulations from this point further.

III. Comparative Results

To estimate the performance of the proposed approximation algorithm, a direct comparison to the theoretical radiation pattern G_{THE} is carried out by calculating the error difference between them (in decibels), according to

$$\mathrm{ERR}(\varphi, \vartheta) = G_{\mathrm{THE}}(\varphi, \vartheta) - \widehat{G}(\varphi, \vartheta). \tag{5}$$

A. Omni-Directional Antennas

In the case of omni-directional antennas, as already mentioned, the radiation pattern is implicitly symmetric around its vertical axis. Therefore, the horizontal cut $\mathrm{hor}(\varphi)$ is equal to 1 for all angles (hence G_H is zero). Consequently, the weight w_1 in (2) is zero and thus, (1) is reducing to $\widehat{G}(\varphi, \vartheta) = G_V(\varphi, \vartheta)$.

Under these conditions, the presented method is equivalent to the classic summing algorithm and the 3-D radiation pattern is perfectly reconstructed, due to its axial symmetry. The technique has been applied successfully to a half-wavelength dipole antenna as well as to a collinear array of two $\lambda/2$ dipoles, for which the theoretical patterns were calculated using typical textbook equations [8].

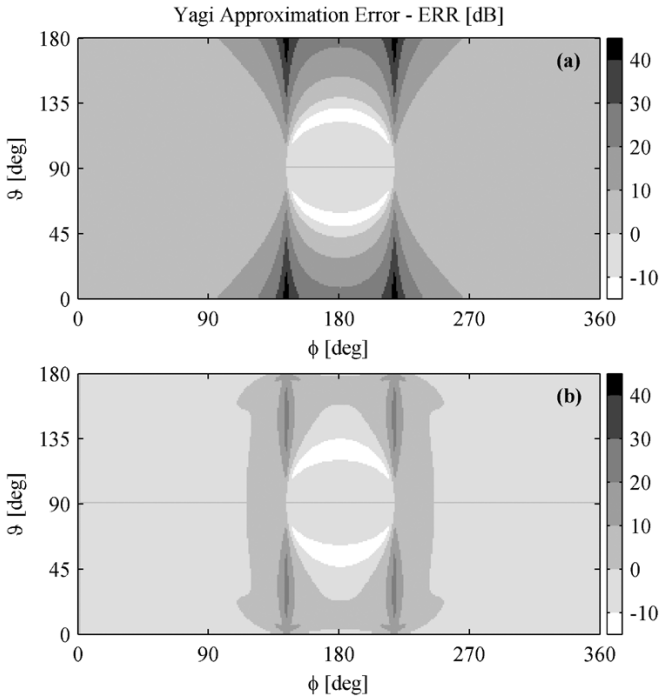

Fig. 3. Approximation error of the 3-element Yagi–Uda array: (a) summing algorithm and (b) proposed algorithm.

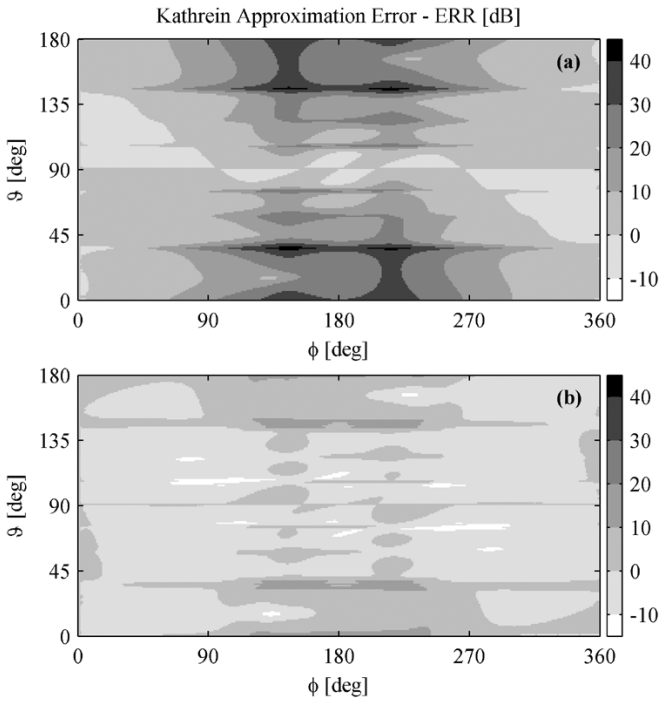

Fig. 4. Approximation error of the Kathrein 739 490 flat panel: (a) summing algorithm and (b) proposed algorithm.

B. Directive Antennas

When directive antennas are considered, the approximation error is lower compared to the summing algorithm. Areas of maximum error are improved, as illustrated in Fig. 3 for the

TABLE I
STATISTICAL EVALUATION OF APPROXIMATION ERROR (PROPOSED METHOD) AND COMPARISON TO SUMMING ALGORITHM (ALL VALUES IN DECIBELS)

Antenna Type	*min*	*max*	μ	$\mu_{abs} \pm \sigma$	μ_n	Summing Algorithm [*min*, *max*] / $\mu_{abs} \pm \sigma$
Omni [a]	0	0	0	0 ± 0	0	[0, 0] / 0 ± 0
Yagi (overall)	–25	24	0	2.4 ± 4	2.2	[–21, 47] / 5.2 ± 7.8
Yagi (sector)	–1	0	–0.2	0.2 ± 0.2	–	[0, 0.1] / 0.01 ± 0.02
Kathrein (overall)	–16	19	–0.8	3.7 ± 3.3	2.9	[–3, 45] / 10 ± 10.1
Kathrein (sector)	–9.6	0.2	–1.9	1.9 ± 2	–	[–0.6, 4.6] / 0.4 ± 0.5

[a]Omni-directional patterns are perfectly reconstructed.

case of a three-element Yagi–Uda array (composed of a driven, a reflecting and a directing element) presented in [9], and in Fig. 4 for a highly directive base-station flat panel (Kathrein 739 490). Theoretical values for the latter array were calculated by rigorous FDTD modeling of the exact antenna geometry. The maxima in these error-plots appear in directions of radiation nulls.

IV. STATISTICAL EVALUATION

For a more thorough examination of these preliminary results, a statistical study has been carried out using typical measures of descriptive statistics. The accuracy is assessed by calculating the range of the error values $[\min, \max]$, their mean value (μ), as well as the mean $(\mu_{\rm abs})$ and standard deviation (σ) of the absolute error. An interesting statistical parameter is the mean absolute error excluding radiation nulls (μ_n), i.e., when $\mathrm{ERR} > 0$ and $G_{\rm THE} < -30$ dBi, then the approximated gain is also a radiation null and thus, no error is accounted.

These measures are calculated over the entire sample set (360×180 values) to evaluate the overall error, as well as in a sector defined by an angular variation of $\pm 60^\circ$ at the horizontal and $\pm 20^\circ$ at the vertical plane, from the antenna's boresight.

Table I summarizes the results of the statistical study. The improvement on the overall mean absolute error, compared to the summing algorithm, is apparent. In fact, when radiation nulls are not taken into account the error is below 3 dB, even for the complex and more directive array (worst case). However, sector-statistics imply that the classic algorithm remains a better solution inside the main radiation sector.

V. HYBRID TECHNIQUE AND OPTIMIZATION

In order to enhance the in-sector performance of the proposed approximation method $\widehat{G}$, a hybrid technique $\widehat{G}_{\rm hyb}$ has been developed and optimized, combining the former with the summing algorithm $G_{\rm SA}$. This is implemented according to

$$\widehat{G}_{\rm hyb}(\varphi, \vartheta) = G_{\rm SA}(\varphi, \vartheta) \cdot w_3 + \widehat{G}(\varphi, \vartheta) \cdot (1 - w_3) \qquad (6)$$

where

$$w_3(\varphi, \vartheta) = \sqrt[n]{\mathrm{hor}(\varphi) \cdot \mathrm{vert}(\vartheta)}. \qquad (7)$$

The product under the radical sign in (7) is actually the normalized decimal (anti-log) radiation pattern, reconstructed using the classic summing algorithm (since logarithmic sum is in fact decimal multiplication). Thus, the weight w_3 represents a function that bridges the two algorithms, depending on the angular direction of interest. Parameter n in (7) can be used to optimize w_3 so that the error becomes minimal. Increasing n is equivalent to relaxing the slope of transitions in the bridging function, therefore allowing more values near the main-lobe to affect the overall gain approximation. The in-sector statistics will thus be improved. However, increasing n will eventually degrade the overall mean error, since larger error values (assigned to the Summing Algorithm) will be involved in the hybrid approximation.

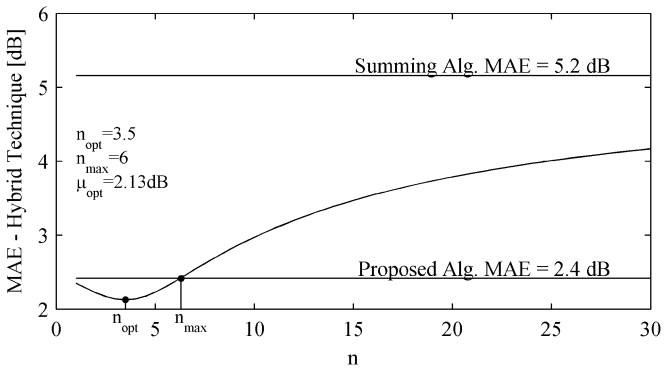

Fig. 5. Parametric study of overall mean absolute error $(\mathrm{MAE} \equiv \mu_{\rm abs})$ using the hybrid approximation technique on the Yagi example array.

This is clearly illustrated in Fig. 5, where the hybrid technique exhibits a minimum at $n_{\rm opt} = 3.5$ $(\mu_{\rm opt} = 2.13\,\mathrm{dB})$, and remains optimized for up to $n_{\max} = 6$. Kathrein in a similar way yields $\mu_{\rm opt} = 3.28\,\mathrm{dB}$ for $n_{\rm opt} = 5$, optimized for up to $n_{\max} = 8.5$. The optimum value of parameter n is associated to the directivity of the antenna under test. The proposed method predicts accurately especially the 3-D radiation patterns of directive arrays, with complex principal patterns. In this study, simulations of patterns with extreme directive characteristics (containing considerably more radiation nulls and side-lobes) have shown that a parameter $n \leq 6$ can provide satisfactory performance for all antenna types.

In order to estimate the efficiency of the proposed technique inside a sector, we have derived statistical contour plots of the mean absolute error $(\mathrm{MAE} \equiv \mu_{\rm abs})$ in sectors of arbitrary size (using optimal n in each antenna case). This is demonstrated in Fig. 6, where areas of higher error tend to minimize in the proposed and hybrid-technique cases (upper right corner of each plot is the overall mean error).

The same effect is illustrated in more detail in Fig. 7 (for the case of the 3-element Yagi–Uda array), where the dark-shaded areas of error between 1 and 3 dB (near $\varphi = 90^\circ$ and 270° in proposed algorithm), almost disappear when the hybrid method is applied.

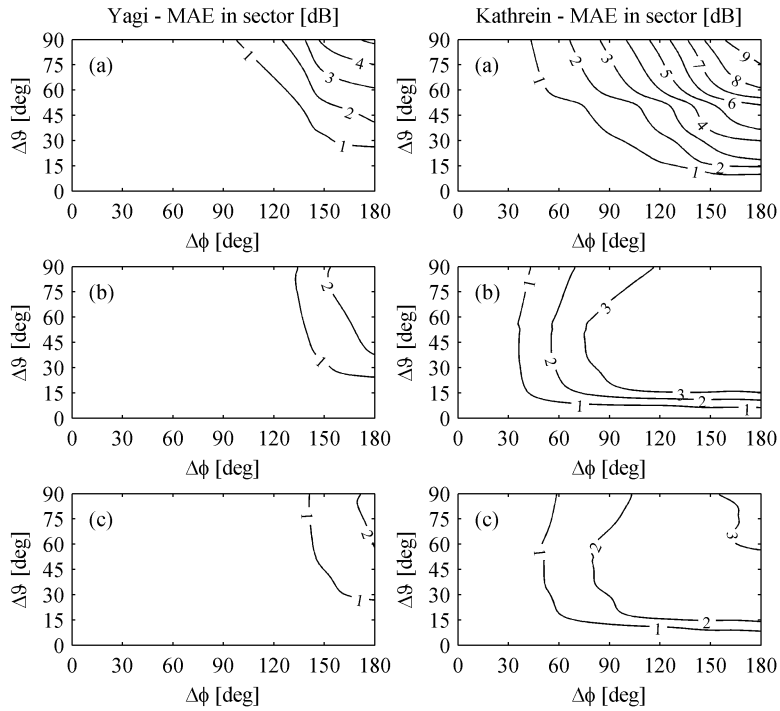

Fig. 6. Mean absolute errors ($\mathrm{MAE} \equiv \mu_{\mathrm{abs}}$) of Yagi and Kathrein, in a sector defined by angular variation $\pm\Delta\phi$ in horizontal and $\pm\Delta\vartheta$ in vertical plane, using (a) summing algorithm, (b) proposed algorithm, and (c) hybrid technique ($n = 3.5$ for Yagi and $n = 5$ for Kathrein).

TABLE II
ANTENNA NOMINAL RADIATION CHARACTERISTICS

Parameter	Kathrein 742 234 (TX)	Kathrein 739 927 (TX)	Electrometrics EM-6952 Log Periodic (RX)
Freq. range (GHz)	1.71-2.17	1.71-1.88	1-18
Gain (dBi)	17.5	19.5	5 @1.8GHz
Horiz. beam-width	66°	33°	70°
Vertical beam-width	7°	9°	125°

VI. EXPERIMENTAL RESULTS

For a practical evaluation of the proposed hybrid approximation method, a set of measurements has been carried out in a realistic scenario using base-station antennas of an existing DCS1800 network. The scenario included the measurement of the actual antenna gain in directions where the aforementioned algorithms yield high approximation errors (worst cases). As pointed out earlier, the pattern reconstruction inside the main-radiation lobe is quite good for all methods, so it was necessary to get measured samples in directions where the azimuth and elevation cuts (that are known for each antenna type) have radiation nulls. To achieve this in the vertical plane, the transmitting antennas must be situated in sufficiently high antenna masts.

The measurements have been carried out at the industrial suburbs of Thessaloniki, using a base-station of Cosmote, a Greek cellular operator. A total of four different flat-panel antenna arrays are installed on this base-station at height $h = 48$ m, forming sectors at different directions, as illustrated in Fig. 8. Measured points were taken on a route (approximately 400 m long) heading north, thus sampling gain values at different pairs of (φ, ϑ) for each antenna. These samples sufficiently cover ranges of (φ, ϑ) lying outside the main-lobe. The antennas under consideration were highly directive arrays manufactured by Kathrein (model 742 234 for #1, 2, 3, and model 739 927 for #4). The principle-plane radiation characteristics of the transmitting and receiving antennas are summarized in Table II.

Each antenna was transmitting on a different DCS broadcast control channel (BCCH) according to the operator's frequency planning for the specific base-station. A pair of (φ, ϑ) is associated to each antenna for every sample point on the measurements' path. The received signal strength (in dBm) was measured on a spectrum analyzer for each BCCH at the points of interest, and further converted into gain using the Friis transmission formula, in order to exclude the distance dependency. These gain values were associated to the corresponding (φ, ϑ)-pair for each antenna separately.

The area surrounding the base-station is characterized as semi-rural. Sparse vegetation and buildings of considerably lower height than the antenna mast were present at distances greater than 40 m from the measurement's path. The propagation conditions can be adequately described by the two-ray model, considering the direct and the ground-reflected ray. In such a case, in the region of 400 m from the transmitters (as the measurement's path total distance) at frequency of approximately 1800 MHz, the path loss exponent is equal to 2, for both vertically and horizontally polarized components [10]. Moreover, since the transmitting antennas were sited significantly higher than the receiving point, the ground-reflection

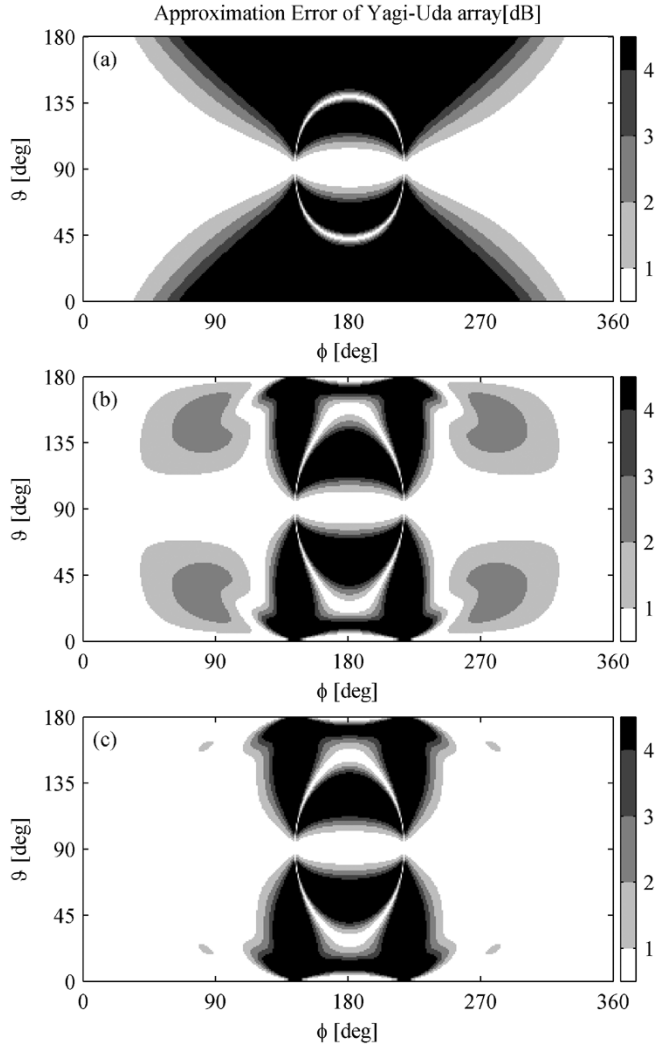

Fig. 7. Absolute approximation errors (in decibels) of Yagi's radiation pattern using (a) summing algorithm, (b) proposed algorithm, and (c) hybrid technique $(n = 3.5)$.

was very close to the directive receiving antenna, ensuring only partial ground-reflection. These propagation conditions (along with line-of-sight between transmitter and receiver) provided a satisfactory approximate of free-space propagation. Thus, a squared-distance dependency (Friis) was assumed.

To eliminate any propagation factors that could potentially affect the gain calculation, due to this approximate modeling of the actual propagation channel by the Friis formula (e.g., ground-reflections that are absent in the ideal free-space channel transmission), a minimum squared error (MSE) fitting algorithm has been applied to the measured data of antenna #1. Thus, an offset parameter (representing all propagation-related uncertainties) was extracted that leads to a best fit between measured and reconstructed normalized gain for this case. This parameter was then used for calculating the measured gain for all other antenna cases, since all broadcast channels were measured consecutively at each point, and therefore exactly the same propagation conditions were applicable at each point for all antennas. The application of this fitting approach is acceptable because, as shown in Fig. 8, the sampled gain values for antenna #1 fall inside the main-lobe (dashed line). In this case, the approximation error (for all antenna types) has been

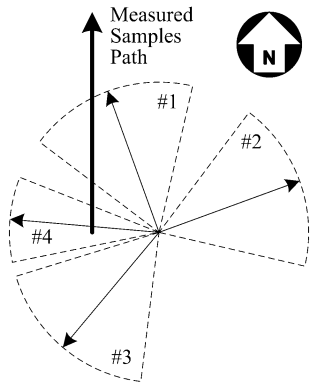

Fig. 8. Antenna mast topology and sector orientation for the base-station used for measurements. Dashed lines represent the half-power beam-width of each sector. Bold arrow-line represents the measurements' route (heading north).

found very low for both the summing algorithm and the hybrid method, and thus negligible differences between them (and the actual measured gain) are expected for antenna #1.

This effect is clearly illustrated in Fig. 9(a), where the dashed line (with triangular markers) representing the summing algorithm's approximated gain, coincides with the solid line (representing the hybrid method's estimated gain). The dotted line (with circular markers) corresponds to the actual measured gain values, which are best-fitted in this case. Values of $\vartheta > 90°$ at the abscissa indicate that all measurements were taken below the antenna's horizon, spanning an interesting range between 95° and 145°. This ensures that measured samples in the elevation pattern sufficiently fall outside the main radiation lobe in the vertical plane, a requirement imposed during the scenario planning.

An overall comparison of the measured normalized gain against the reconstructed gain obtained using the summing algorithm and the proposed hybrid technique is also depicted in Fig. 9, for the other antennas on the base-station under consideration.

VII. Discussion

From the topics discussed so far, it is shown that the error introduced in the propagation prediction process is very high in some cases (reaching 50 dB) for the existing techniques, which results in misleading predictions for the overall wireless system coverage. The significance of accurate reconstruction of antenna radiation patterns is crucial for system planning, especially in microcell or picocell network configurations, where excessive traffic is expected and redundant cells are required for increased capacity. Additionally, in those cases, the exact knowledge of each cell's boundaries is needed to minimize interference between them and to optimize traffic serving.

For example, antenna beam-tilting and back-lobe servicing are some common features that are often used in high capacity wireless systems, in order to accommodate more traffic (or to minimize interference). Moreover, in small-cell configurations the gain must be adequately accurate at elevation angles very close to the antenna (far below the horizon), due to the restricted cell-size. The latter also applies in cases where directional antenna arrays are used horizontally (in a way such that their elevation pattern is used in the horizontal plane), creating narrow

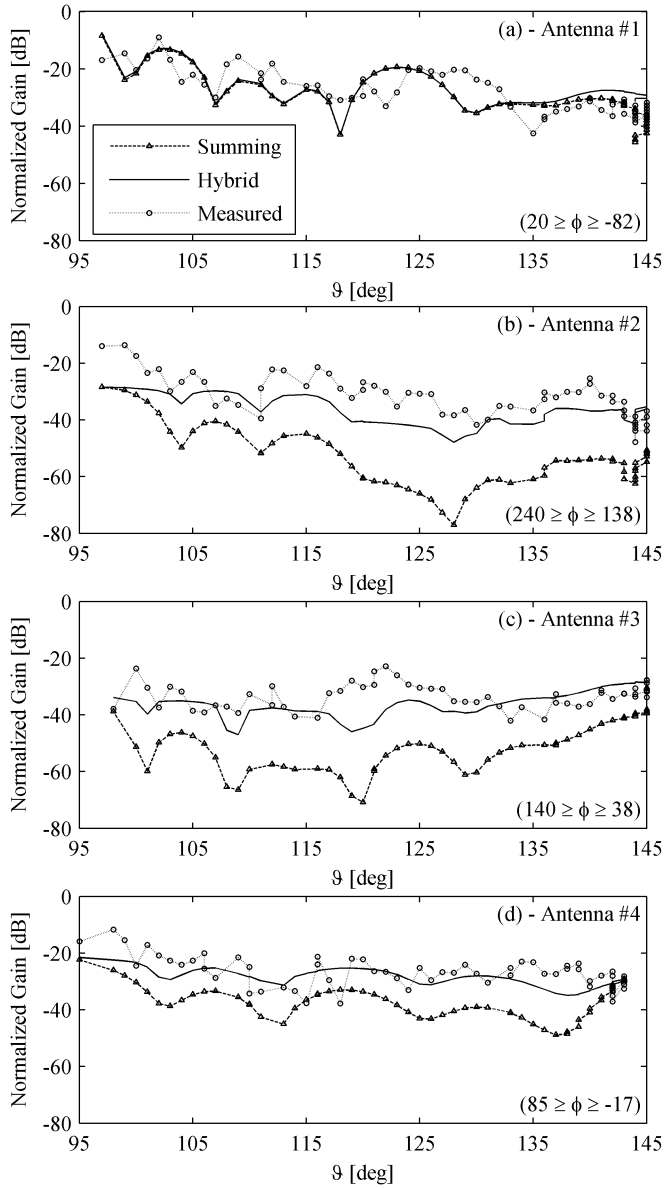

Fig. 9. Comparison plots between measured and approximated normalized gain, for each antenna case ($n = 5$). Abscissa is the elevation angle ϑ, from the (φ, ϑ)-pair of each measured point (range of associated azimuth angles is in parentheses). The legend applies to all plots.

slice-cells. In this case (used for example in stadiums hosting crowded athletic events), the exact cell boundaries are very important since each cell is designed for maximum capacity and should not accept additional traffic from adjacent cells. Therefore, the estimated antenna pattern has to be accurate enough, also in areas outside the main radiation lobe.

The pattern reconstruction technique proposed in this paper provides lower approximation error than other methods found in literature or the classic summing algorithm, as already illustrated in Figs. 3 and 4. The hybrid technique extends even further the performance of the proposed method near the main radiation sector, as shown in Figs. 6 and 7.

Mean absolute error statistics presented in Table I, prove that an average error of 2–3.5 dB is typical for the directive (worst case) antennas examined herein. This error remains below 3 dB if radiation nulls are excluded from the statistical study. The corresponding standard deviation was 3–4 dB. Moreover, omni-directional antennas are perfectly reconstructed as required by their axial symmetry. The average error (taking into account the sign of the error difference) is below 1 dB, calculated over the entire sample-set, with error values extending symmetrically over the entire $[\min, \max]$ range (Table I).

This effect indicates that points of overestimated antenna gain (having negative error difference) are fairly equal to the points of underestimated gain (positive error difference). This unbiased behavior is desirable in designing the reconstruction algorithm, since both cases are important during system coverage planning. That is, overestimated gain can lead to inadequate cell coverage, while underestimated gain leads actually to overlapping and interfering cells. Note that the summing algorithm tends to underestimate the antenna gain, as shown in Table I, Figs. 3 and 4 (greater positive error).

Except for the advantages of the hybrid technique that were presented earlier on a theoretical basis (by simulating several antenna types), the accuracy of the proposed approximation algorithm has been also revealed by a set of measurements performed on antennas of a real DCS1800 base station. As illustrated in Fig. 9, the gain calculated using the hybrid technique appears to have a better match with the actual measured antenna gain (for all cases where the two approximation methods significantly differ from each other), as shown in Fig. 9(b)–(d).

The two methods predict different approximations in these cases, because the set of measured points is outside the main radiation sector of each antenna, with associated (φ, ϑ)-pairs in areas where the hybrid technique performs better than the summing algorithm. More specifically, the measured samples for antenna #1 are associated to elevation angles ranging from 145° down to 95° with respective azimuth angles ranging between $-82°$ and 20° (including the main radiation sector). In contrast, for the case of antenna #2 the azimuth angles of the measured points vary from 138° to 240° (far beyond the main-lobe). Similarly, for antenna #3 the samples are ranging in azimuth angles of 38°–140°. Finally, the measured samples for antenna #4 are associated to azimuth angles from $-17°$ to 85°. In this case all the samples are falling outside the horizontal or the vertical main-lobe. Moreover, this model has narrower nominal beam-width (as shown in Fig. 8) compared to the previous cases. This antenna behaves in a similar way to the previous cases (#2 and #3) and therefore some divergence is again observed between the compared methods.

Measured gain in Fig. 9 fluctuates because of multipath effects during the measurements, mainly caused by partial ground-reflections as well as by scattering from sparse vegetation and low-height buildings surrounding the base-station. However, the tendency of the measured gain curve is sufficiently indicative of the accuracy achieved by the proposed hybrid technique in approximating the antenna's radiation pattern, compared to the summing algorithm.

VIII. Conclusion

A novel technique for reconstructing the 3-D radiation pattern of antennas has been presented in this paper. In pursuit of an even more accurate estimate for the radiation solid of directive antenna arrays, an improvement of at least 3 to 7 dB in mean

absolute approximation error, compared to the classic summing algorithm that is being extensively used nowadays, could be significant in the network planning process or the system's cell coverage prediction, as discussed.

Moreover, the proposed hybrid algorithm has zero approximation error when used for reconstructing omni-directional patterns. In the case of directive antennas the absolute error remains lower than other reconstruction techniques presented in literature. In addition, the proposed method exhibits an unbiased statistical error behavior, thus remaining generally neutral in the estimation of the reconstructed 3-D radiation pattern.

Finally, the performance of the developed algorithm has been practically evaluated through a realistic measurements' scenario, in which the approximated gain of four different base-station antennas has been compared against the measured gain in each case. The result of this comparison has proved that the proposed hybrid algorithm provides a considerably more accurate estimate of the actual antenna gain than the classic summing algorithm.

Inside the area of the main radiation sector of each antenna, both the summing algorithm and the proposed hybrid technique provide similarly accurate pattern approximations, achieving comparably low absolute errors of mean value and standard deviation below 0.5 dB.

ACKNOWLEDGMENT

The authors would like to thank Greek cellular operator Cosmote S. A., Radio-networks Division, Department of Network-Performance Monitoring & New Technologies, for providing all necessary information about the base-station antennas, in order to conduct the measurements presented in this paper.

REFERENCES

[1] R. R. Skidmore, "A Comprehensive In-Building and Microcellular Wireless Communication System Design Tool," M.S. thesis, Dept. Elect. Eng., Virginia Polytechnic Inst. and State Univ., Blacksburg, VA, 1997.

[2] F. Gil, A. R. Claro, J. M. Ferreira, C. Pardelinha, and L. M. Correia, "A 3-D extrapolation model for base station antennas' radiation patterns," in *Proc. IEEE Vehicular Tech. Conf., VTC Fall*, vol. 3, 1999, pp. 1341–1345.

[3] ——, "A 3-D interpolation method for base-station-antenna radiation patterns," *IEEE Antennas Propag. Mag.*, vol. 43, no. 2, pp. 132–137, Apr. 2001.

[4] R. J. Allard and D. H. Werner, "The simultaneous interpolation of antenna radiation patterns in both the spatial and frequency domains using model-based parameter estimation," *IEEE Trans. Antennas Propag.*, vol. 48, no. 3, pp. 383–392, Mar. 2000.

[5] ——, "The model-based parameter estimation of antenna radiation patterns using windowed interpolation and spherical harmonics," *IEEE Trans. Antennas Propag.*, vol. 51, no. 8, pp. 1891–1906, Aug. 2003.

[6] W. T. A. Lopes, G. Glionna, and M. S. de Alencar, "Generation of 3-D radiation patterns: A geometrical approach," in *Proc. IEEE Vehicular Tech. Conf., VTC Spring*, vol. 2, 2002, pp. 741–744.

[7] F. Mikas and P. Pechac, "The 3-D approximation of antenna radiation patterns," in *Proc. Inst. Elect. Eng. 12th Int. Conf. Antennas Propagat., ICAP*, 2003, pp. 751–754.

[8] C. A. Balanis, *Antenna Theory: Analysis and Design*, 2nd ed. New York: Wiley, 1997, pp. 157–164.

[9] K. Siwiak, *Radiowave Propagation and Antennas for Personal Communications*, 2nd ed. Norwood, MA: Artech House, 1998, pp. 57–61.

[10] S. R. Saunders, *Antennas and Propagation for Wireless Communication Systems*. Chichester, U.K.: Wiley, 1999, pp. 253–255.

Theodore G. Vasiliadis (S'99) was born in Kozani, Greece, in 1977. He received the Diploma degree in electrical and computer engineering from Aristotle University of Thessaloniki, Greece, in 1999. He is currently working toward the Ph.D. degree at the Telecommunications Laboratory, Department of Electrical and Computer Engineering, Aristotle University of Thessaloniki.

Since 1999, he has been involved in several research projects dealing with wireless systems' design/modeling, propagation modeling/measurement, and high-capacity microcellular networks' design (Athens 2004 Olympics). At the same time, he worked as a Research and Teaching Assistant at the Aristotle University. His research interests include propagation modeling, microwave antenna design, modeling and prototyping, as well as phased antenna arrays.

Mr. Vasiliadis is a Member of the European Microwave Association (EuMA) and the Technical Chamber of Greece.

Antonis G. Dimitriou (S'01) was born in Ierapetra, Greece, in 1977. He received the Diploma in electrical and computer engineering from the Aristotle University of Thessaloniki, Greece, in 2001, where he is working toward the Ph.D. degree.

Since 2001, he has been a Teaching and Research Assistant in the Department of Electrical and Computer Engineering of the Aristotle University of Thessaloniki, where he has participated in numerous research activities, including the design of a GSM cellular network inside the Olympic Stadium for the 2004 Olympic Games. His current interests are in the areas of antennas, propagation modeling, using high frequency methods in electromagnetics and planning.

Mr. Dimitriou is a Member of the Technical Chamber of Greece.

George D. Sergiadis (M'88) was born in Thessaloniki, Greece, in 1955. He received the Diploma degree in electrical engineering from the Aristotle University of Thessaloniki, Greece, in 1978, and the Ph.D. degree from "Ecole Nationale Supérieure des Télécommunications," Paris France, in 1982.

He worked with Thomson CsF, in France, until 1985, participating in the development of the French Magnetic Resonance Scanner. Since 1985, he has been with the Aristotle University of Thessaloniki, Greece, teaching Telecommunications and Biomedical Engineering, now as an Associate Professor. For three years he served also as the Director of the Telecommunications Department. He developed the Hellenic TTS engine "Esopos," and designed the mobile communications for the Athens Olympic Games in 2004. From 2004 to 2005 he was on sabbatical at the Media Laboratory, Massachusetts Institute of Technology, Cambridge. His current research interests include fuzzy image processing and wireless communications.

Dr. Sergiadis is the President of ELEVIT, the Hellenic society for Biomedical Engineering, and a Member of the Technical Chamber of Greece, ATLAS, SMRM, ESMRM, EMBS, and SCIP.